*Int. J. Electrochem. Sci.*, 17 **(2022)** Article Number: 220125, doi: 10.20964/2022.01.39

International Journal of
ELECTROCHEMICAL
SCIENCE
www.electrochemsci.org

# Incorporation of $Co^{2+}$, $Cu^{2+}$, and $Zn^{2+}$ ions into nickel oxide thin films and their enhanced electrochemical and electrochromic performances

*Kyung Ho Kim*[1,*], *Sho Fujii*[2], *Yoshio Abe*[1]

[1] School of Earth, Energy and Environmental Engineering, Kitami Institute of Technology, 165 Koen-cho, Kitami, Hokkaido 090-8507, Japan
[2] Department of Natural Sciences, National Institute of Technology, Kisarazu College, 2-11-1 Kiyomidai Higashi, Kisarazu, Chiba 292-0041, Japan
[*]E-mail: khkim@mail.kitmai-it.ac.jp

*Received:* 2 October 2021 / *Accepted:* 10 November 2021 / *Published:* 6 December 2021

Nickel oxide (NiO) thin films incorporating cobalt (Co), copper (Cu), and zinc (Zn) dopants were prepared using a simple and cost-effective sol-gel spin-coating method. Changing the dopant allowed the color of the NiO thin films to be tuned. Cracking on the surface of the NiO thin films was effectively reduced by the incorporation of dopants. The undoped NiO and Co-doped NiO thin films had a relatively porous nanoparticle structure, whereas the Cu-and Zn-doped NiO thin films had a more compact nanoparticle structure. Compared with the undoped NiO sample, the cyclic voltammetry (CV) curves of the doped NiO thin films exhibited higher integrated current densities. In particular, the CV curves of the Co-doped NiO thin film showed no symmetric distortion as the scan rate increased, indicating a highly reversible redox process. At a scan rate of 5 mV/s, the calculated areal specific capacitance was 19.7 mF/cm$^2$, and it showed excellent cycling stability at high scan rate (~88% retention at 100 mV/s after 2000 cycles). The color of the Co-doped NiO thin film changed from pale pink (bleached state) to brown (colored state). Co doping demonstrated great potential for improving the electrochemical and electrochromic performance of NiO thin film, while also offering long-term stability and enhanced optical modulation.

**Keywords:** NiO, Thin film, Electrochemical stability, Electrochromic performance

## 1. INTRODUCTION

Owing to the wide applicability of nanostructured nickel oxide (NiO) thin films, multiple studies have been conducted to optimize the solution-based preparation methods, which are noted for their simplicity, cost-effectiveness, and reliability [1-5]. In addition, doping is recognized as an effective way

to improve the catalytic and magnetic performance of NiO [3-5]. Ethiraj investigated the characteristics of Cu-doped NiO nanoparticles synthesized by a wet chemical method as an effective photocatalyst for phenol degradation [3], while Ponnusamy reported that chemically synthesized Co-doped nanoparticles exhibited ferromagnetic behavior at room temperature [4]. Alternatively, Panigrahi reported that Zn-doped NiO nanoparticles synthesized using a wet chemical method have strong potential for multifunctional applications such as ultraviolet emission devices, random access memory, and data storage applications [5]. In addition, NiO nanoparticles prepared via the hydrothermal precipitation method exhibit reliable electrochemical capacitive behavior, thus showing potential as active electrode materials [6,7]. Moreover, unlike conventional active electrode fabrication methods based on synthesized nanoparticles, thin films prepared directly on conductive substrates are simpler to fabricate because no additional processing involving conductive agents such as black carbon or polymer binders such as polytetrafluorothylene (PTFE) is required [8]. Furthermore, directly prepared NiO thin films can also be used as electrochromic materials for energy-efficient window applications [9].

In this study, we prepared NiO thin films with various dopants (Co, Cu, Zn) using sol-gel spin-coating and compared their morphological, electrochemical, and electrochromic properties with undoped NiO thin film. Our discussion focuses primarily on the effect of high dopant concentrations on the properties of NiO thin film. In addition, efficient electrochromic films based on electrochemically stable NiO offer a solution to the energy crisis and can be used in sustainable applications.

## 2. EXPERIMENTAL

To prepare the undoped NiO thin film, nickel acetate tetrahydrate ($Ni(CH_3COO)_2 \cdot 4H_2O$, 0.5 M) was dissolved in 2-methoxyethanol (2ME, $C_3H_8O_2$). After stirring at 60 °C for 1 h, it was aged at room temperature for 24 h. After spin-coating, the samples were dried at 150 °C for 10 min before being annealed at 300 °C for 1 h in air. To prepare doped NiO thin films, nickel acetate tetrahydrate ($Ni(CH_3COO)_2 \cdot 4H_2O$, 0.4 M) and one of cobalt acetate tetrahydrate ($Co(CH_3COO)_2 \cdot 4H_2O$, 0.1 M), copper acetate monohydrate ($Cu(CH_3COO)_2 \cdot H_2O$, 0.1 M), or zinc acetate dihydrate ($Zn(CH_3COO)_2 \cdot 2H_2O$, 0.1 M) were dissolved in 2ME. The spin-coating, drying, and annealing processes were repeated under the same conditions used to prepare the undoped sample.

The crystallinity of the various thin films was determined using X-ray diffraction (XRD, D8ADVANCE). Optical transmittance spectra were obtained using ultraviolet-visible spectroscopy (HITACHI, U-2910). The chemical bonding states were identified via Fourier transform infrared spectroscopy (FTIR, FT/IR-6100) and X-ray photoelectron spectroscopy (XPS, JPS-9200) using a Mg-Kα X-ray source. The surface morphologies were analyzed using field emission scanning electron microscopy (FESEM, JSM-6701). Cyclic voltammetry (CV) measurements were performed using a three-electrode system in which the NiO thin films were prepared on fluorine-doped tin oxide (FTO) as the working electrode, with Pt as the counter electrode and Ag/AgCl as the reference electrode, in a 1 M KOH aqueous electrolyte. *In-situ* optical transmittance spectra were measured using a charge-coupled device multichannel detector (USB2000+, Ocean Optics) with halogen and deuterium lamps; air and a quartz-glass cell filled with 1 M KOH were used as references [10].

## 3. RESULTS AND DISCUSSION

As shown by the XRD patterns in Fig.1(a), all samples prepared on glass substrates exhibited diffraction peaks at $2\theta$ positions of 37.3º and 43.3º, which were indexed to the (111) and (200) planes of the cubic phase of NiO (JCPDS No. 04-0835), respectively. The weak intensity and broadness of the diffraction peaks indicate nanocrystalline NiO. No secondary diffraction peaks associated with an oxide phase (metal or otherwise) were observed. The most likely reason for this is the high solid solubility of Co, Cu, and Zn in NiO [11-13]. The FTIR spectra (Fig.1(b)) show that the NiO samples all exhibit a strong absorption peak at ~400 $cm^{-1}$, which corresponds to the Ni-O stretching vibration. A broad and weak absorption peak exists at ~3400 $cm^{-1}$, which corresponds to stretching hydroxyl groups in the hydrogen-bonded vibration of water [6]. Figure 1(c) shows the optical transmittance spectra of NiO thin films prepared on FTO/glass substrates with various dopants. Incorporating different dopants enables the sample color to be tuned. For example, Zn doping results in the absorption edge shifting slightly toward shorter wavelengths, while the average transmittance is also higher than that of the other samples. The potential of highly transparent Zn-doped NiO thin film as hole transport layer in perovskite solar cells has been highlighted in a previous report [14]. The Co- and Cu-doped NiO samples displayed a slightly reddish color and the undoped NiO sample was light gray.

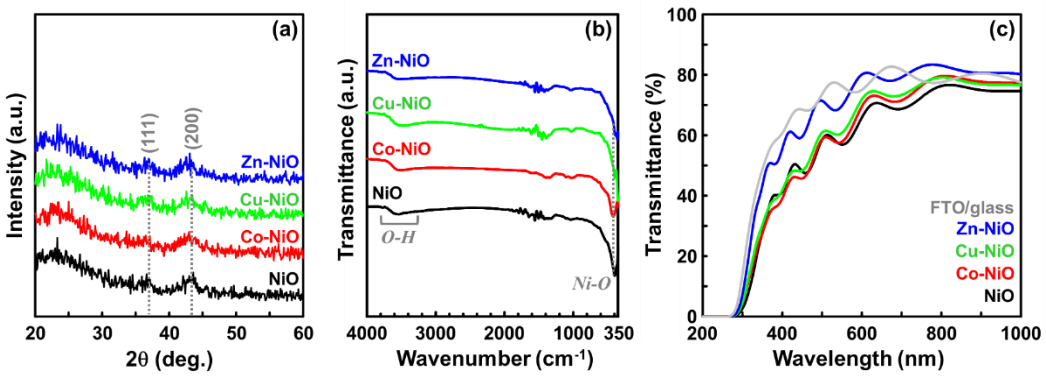


**Figure 1.** XRD patterns (a), FTIR spectra (b), and optical transmittance spectra (c) of the NiO thin films with different dopants.

The XPS profiles in Fig.2(a) show that all samples had characteristics Ni $2p_{3/2}$ and Ni $2p_{1/2}$ peaks at ~853.5 and ~871.4 eV, respectively, which is well agreement with other report [15]. Incorporating dopants led to the emergence of the corresponding 2*p* peaks for Co, Cu, or Zn [15,16], indicating the presence of $Co^{2+}$, $Cu^{2+}$, or $Zn^{2+}$ cations in the NiO thin films (Fig.2(b-d)). The O 1*s* spectra of undoped, Co-, Cu-, and Zn-doped NiO samples are shown in Fig.2(e-h), respectively. The peaks were fitted using three different species of oxygen at the binding energies of ~529.3, ~521.2, and ~532.5 eV, which are associated with metal-bonded oxygen (O1), low-coordination oxygen defects (O2), and physisorbed and chemisorbed oxygen in water on the sample surface (O3), respectively [15]. The O2/O1 ratios of the doped-NiO samples were slightly higher than that of the undoped NiO sample, implying that doping benefits the electrochemical performance of NiO thin films [15].

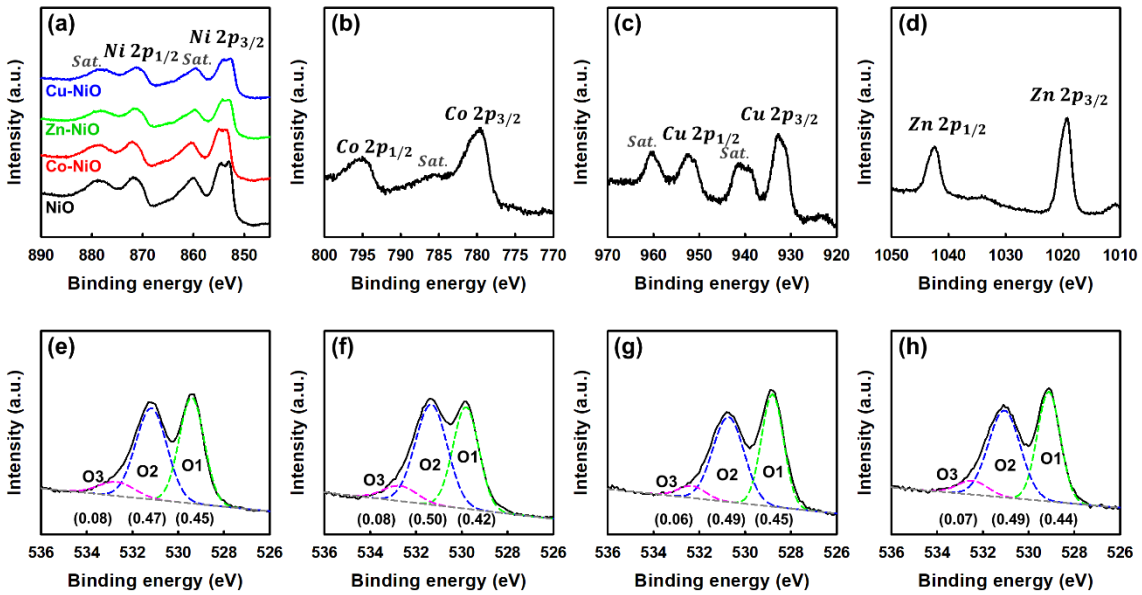


**Figure 2.** XPS profiles of the NiO thin films; Ni 2p (a), Co 2p (b), Cu 2p (c), Zn 2p (d), O 1s (e-h); NiO (e), Co-NiO (b,f), Cu-NiO (c,g), Zn-NiO (d,h) thin films.

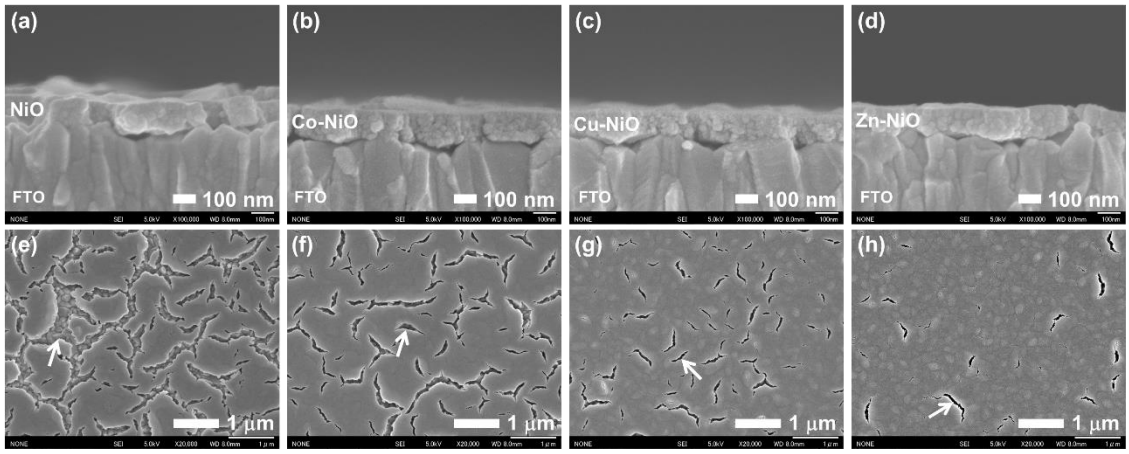


**Figure 3.** FESEM images of NiO (a,e), Co- (b,f) , Cu- (c,g), and Zn- (d,h) doped NiO thin films; (a-d) top images, (e-h) cross-sectional images.

Figure 3 shows the FESEM images of the NiO thin films prepared on FTO/glass substrates. The cross-sectional images in Fig.3(a-d) show that the thickness of the thin films is approximately 120 nm, with each film composed of nanoscale particles. This nanoparticle structure could be beneficial for electrolyte penetration, leading to improved electrochemical performance [2]. As shown in Fig.3(e-h), cracks, indicated in the images by arrows, were observed on the surface of each thin film sample. However, doping was found to decrease the number of cracks, with Zn proving the most effective dopant in terms of crack reduction. The surface coverage was determined to be approximately 80, 87, 94, and 97% for undoped and the Co-, Cu-, and Zn-doped NiO samples, respectively. These results might be due

to the differences in ion radius between $Ni^{2+}$ (0.069 nm) and the dopants ($Co^{2+}$ (0.072 nm), $Cu^{2+}$ (0.073 nm), $Zn^{2+}$ (0.074 nm)) [17,18]. The reduction in crack formation for the doped samples might be caused by the dopant alleviating stress between NiO thin films and FTO.

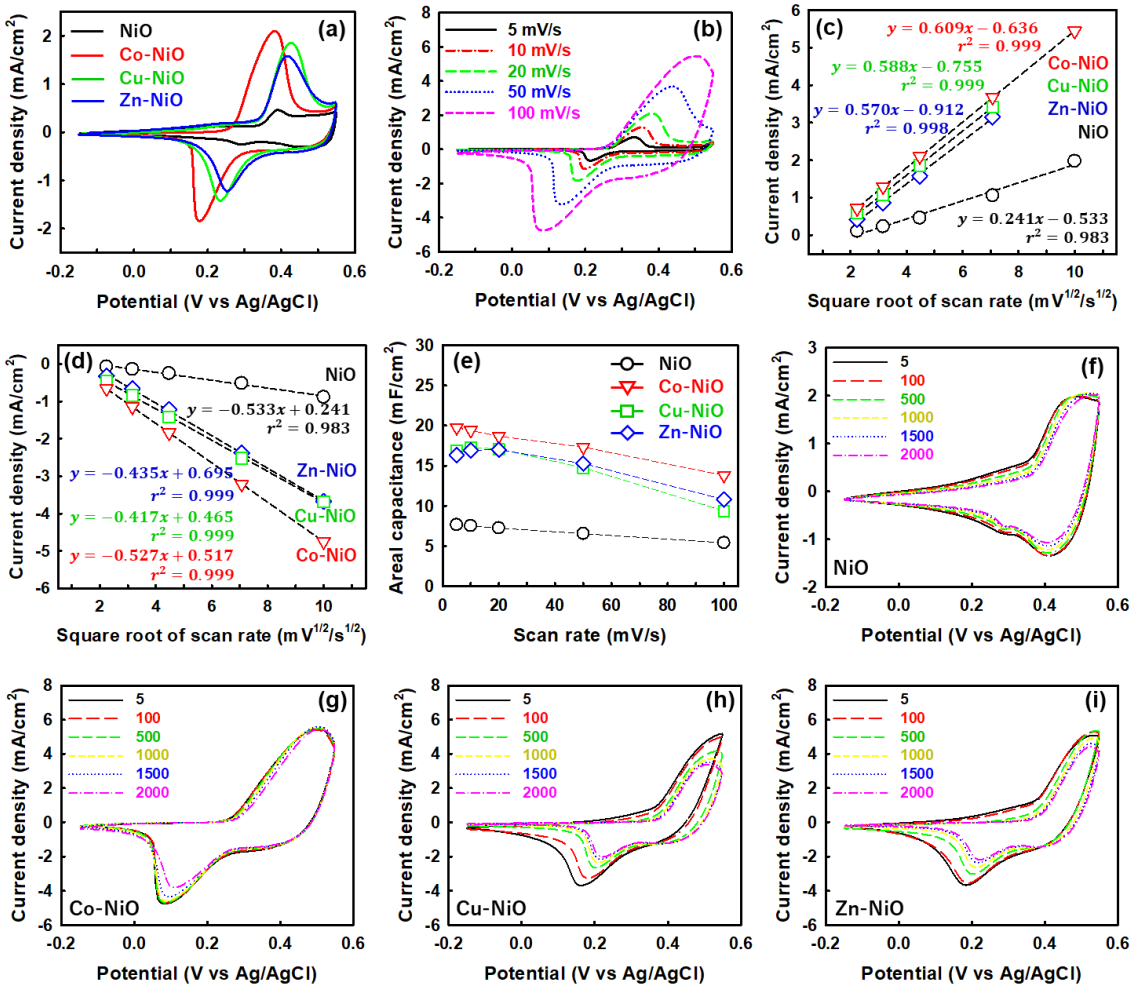


**Figure 4.** CV curves of NiO samples with various dopants at a scan rate of 20 mV/s (a), CV curves of the Co-doped NiO sample at various scan rates (b), current densities of the anodic and cathodic peaks obtained from the CV curves as a function of the square root of the scan rate (c,d), areal specific capacitances (e), and CV curves at a scan rate of 100 mV/s with cycling (f-i); NiO (f), Co-NiO (g), Cu-NiO (h), Zn-NiO (i).

The performance of the electrochemical capacitors was evaluated via CV measurements [19], which were conducted between −0.15 and +0.55 V after exposing the thin film samples to ozone. Figure 4(a) shows the CV curves of NiO samples with various dopants at a scan rate of 20 mV/s. Similar CV curve profiles were observed for all samples, which indicates pseudo-capacitance behavior from Faradaic processes [20]. Each CV curve exhibited a pair of strong anodic and cathodic redox peaks, which can be attributed primarily to the reversible faradic redox behavior of $Ni^{2+} \leftrightarrow Ni^{3+}$ [20]. Moreover, the potential of the redox peak depends strongly on the dopant. For example, relative to the redox peaks of the undoped NiO sample, those of the Co-doped NiO sample were shifted to the negative potential

region, which can be attributed to the lower redox potential of Co-based systems relative to their Ni-based counterparts [21]. Furthermore, the Cu- and Zn-doped NiO samples both showed a positive shift in the oxidation peak potential and a negative shift in the reduction peak potential [22,23]. Overall, the CV curves show that the doped NiO samples possess a larger integral area and higher redox current density compared with the undoped NiO sample.

Figure 4(b) shows the CV curves of the Co-doped NiO sample at various scan rates from 5 to 100 mV/s. As the scan rate increases, the current density increases, and the anodic and cathodic peaks shift toward the positive and negative potential regions, respectively. The CV curves of the Co-NiO sample retain their shape as the scan rate increases. As shown in Fig.4(c,d), the current densities of the anodic and cathodic peaks are proportional to the square root of the scan rate, indicating diffusion-limited redox reactions [21]. Further, the gradients of the Co-doped NiO sample were steeper than those of the other samples, implying an elevated rate of charge transfer and ion diffusion [24].

Figure 4(e) shows the areal specific capacitances calculated from the CV curves. At all scan rates, the Co-doped NiO sample exhibited higher capacitance values than the others. Capacitance values of 19.7, 19.4, 18.7, 17.3 and 13.8 mF/cm$^2$ were calculated at scan rates of 5, 10, 20, 50, and 100 mV/s, respectively. The capacitance value is shown to decrease with an increase in the scan rate because of the reduced rate of electrolyte transport [6,25]. Nevertheless, the Co-doped NiO sample demonstrates an impressive high-rate capability owing to its porous nanoparticle structure (~70% of capacity retention at 100 mV/s), which is a key parameter for satisfying the high power demands of energy storage devices [26]. Significantly, the Co-doped NiO sample outperformed alternative inexpensive transition oxide electrode material (e.g., copper oxide (CuO), 0.12 mF/cm$^2$) [19].

Figure 4(f-i) shows the CV curves at a scan rate of 100 mV/s with cycling. The electrochemical cycling stability is critical for practical applications. The CV curves of the Co-doped NiO sample show no pronounced distortion during cycling, and exhibit excellent cycling stability: ~88% retention over 2000 cycles. Although the Cu- and Zn-doped NiO samples also demonstrate high current densities, they show relatively poor retention (~56%). A possible explanation for this is the peak shifts resulting from the redox reaction, while the compact morphologies of the Cu- and Zn-doped NiO samples mean that there is insufficient time for the reaction to proceed at higher scan rate [6,26,27]. Compared with the other samples, the Co-doped NiO sample, which has a relatively porous structure, exhibits a promising electrochemical performance, including cycling durability at a high scan rate.

Figure 5 (a) shows the electrochromic performance of the Co-doped NiO sample at a scan rate of 100 mV/s within a potential window between −0.15 and +0.55 V. Based on the variation of the *in-situ* transmittance at a wavelength of 500 nm, the transmittance change ($\Delta T$) and optical density change ($\Delta OD$) recorded at the 30$^{th}$ (420 s), 1000$^{th}$ (14000 s), and 2000$^{th}$ (28000 s) cycle were ~40% and 0.44, ~36% and 0.43, and ~35% and 0.43, respectively. The decrease in transmittance after 2000 cycles was only ~12%, indicating excellent sustainability compared with other reported NiO film prepared by the precipitation method (e.g., 61% decrease after 2000 cycles) [28]. The *in-situ* transmittance spectra of the Co-doped NiO sample, which were measured for 18 s under an applied potential of −0.15 V and for 18 s at +0.55 V, are shown in Fig.5(b). The corresponding photographs show that the color of the sample changes from pale pink (bleached) to brown (colored). The optical switching time measured at a wavelength of 500 nm was ~4 s for bleached ($t_b$) and ~2 s for colored ($t_c$) states (Fig.5(c)), which is

comparable to porous nanowall-structured NiO prepared by chemical bath deposition ($t_b$ 2.9 s, $t_c$ 3.5 s) [29]. These results indicate that the Co-doped NiO sample represents a promising electrochromic thin film with excellent cycling durability.

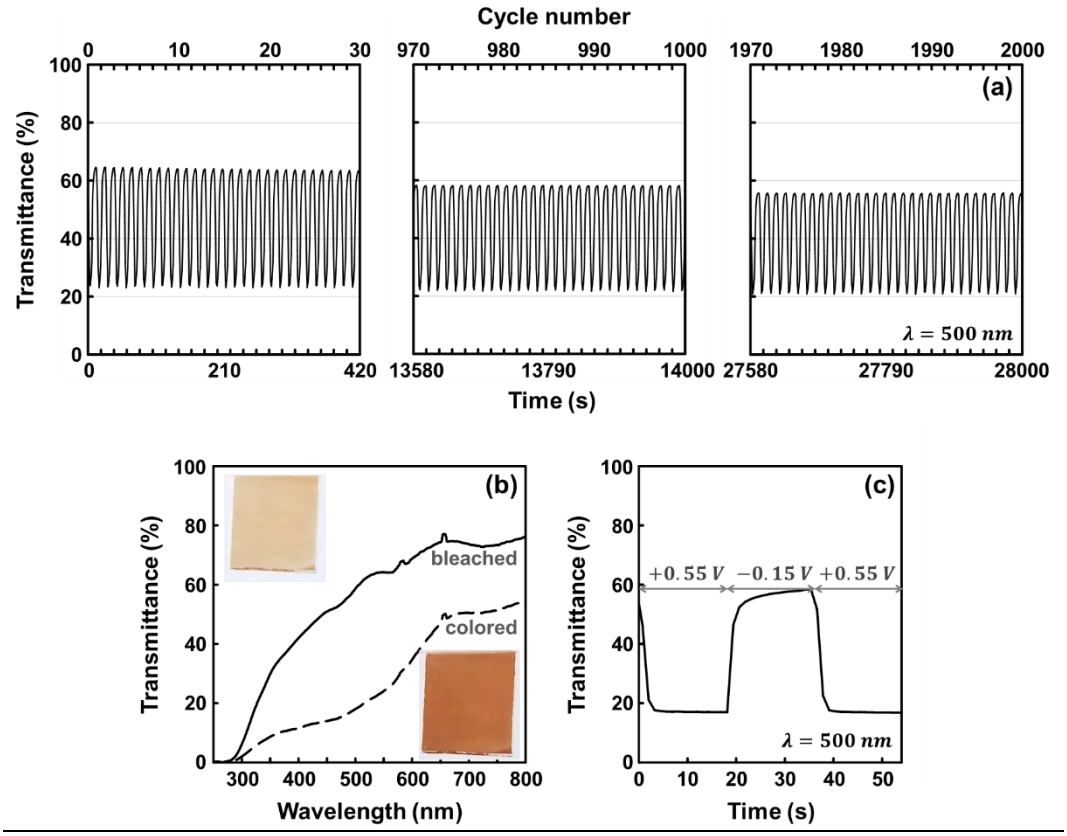


**Figure 5.** Variations in the *in-situ* transmittance of Co-doped NiO sample at a scan rate of 100 mV/s during cycling (a), *in-situ* transmittance spectra for the colored and bleached states (b), and variation in the *in-situ* transmittance at a wavelength of 500 nm with time (c).

## 4. CONCLUSIONS

We investigated the effects of Co, Cu, and Zn dopants on the optical, morphological, electrochemical, and electrochromic properties of NiO thin films prepared via sol-gel spin-coating. The XPS results confirmed that the NiO was doped with Co, Cu, and Zn. The Co- and Cu-doped NiO thin films were slightly reddish, whereas the Zn-NiO thin film was highly transparent over the visible wavelength region. All the NiO thin films were composed of nanoparticles, and exhibited increased surface coverage compared with the undoped sample to incorporate the Co, Cu, and Zn dopants. In addition, the CV measurements indicated that each NiO sample exhibited a strong faradaic reaction, with the symmetric characteristic of the redox peaks suggesting high reversibility. Moreover, the redox peaks shifted as the composition of the electrode materials changed. The Co-doped NiO sample demonstrated excellent long-term electrochemical stability, retaining a capacity of ~88% after 2000 cycles, representing a notable improvement compared with the values of ~70, ~56, and ~56% recorded for the undoped, Cu-, and Zn-doped NiO, respectively. These results validate the high optical modulation, fast

optical switching time, and excellent cycling durability of Co-doped NiO compared with undoped NiO. As such, this simple-to-prepare Co-doped NiO thin film represents an attractive material for applications requiring high-performance supercapacitors with efficient electrochromic performance.

ACKNOWLEDGEMENT
This study was supported by KNIT Collaborative Research Fund. The authors would like to thank Susumu Tokuda of the Open Facility Center of the Kitami Institute of Technology for his assistance with FESEM characterization and Ayano Yamazaki of Open Facility Division, Global Facility Center, Creative Research Institution, Hokkaido University for performing XPS measurements.

## References

1. R.S. Kate, S.A. Khalate and R.J. Deokate, *J. Alloys Compd.,* 734 (2018) 89.
2. D.S. Dalavi, R.S. Devan, R.S. Patil, Y.R. Ma and P.S. Patil, *Mater. Lett.,* 90 (2013) 60.
3. A.S. Ethiraj, P. Uttam, V. K, K.F. Chong and G.A.M. Ali, *Mater. Chem. Phys.,* 242 (2020) 122520.
4. P.M. Ponnusamy, S. Agilan, N. Muthukumarasamy and M. Raja, *J. Mater. Sci: Mater. Electron.,* 27 (2016) 399.
5. U.K. Panigrahi, P.K. Das, R. Biswal, V. Sathe, P.D. Babu, A. Mitra and P. Mallick, *J. Alloys Compd.,* 833 (2020) 155050.
6. T. Meng, P-P. Ma, J-L. Chang, Z-H. Wang and T-Z. Ren, *Electrochim. Acta,* 125 (2014) 586.
7. V.S. Reddy Channu, R. Holze and B. Rambabu, *Colloids Surf. A Physicochem. Eng. Asp.,* 414 (2012) 204.
8. X.L. Guo, X.Y. Liu, X.D. Hao, S.J. Zhu, F. Dong, Z.Q. Wen and Y.X. Zhang, *Electrochim. Acta,* 194 (2016) 179.
9. C.G. Granqvist, *Thin Solid Films,* 564 (2014) 1.
10. Y. Abe, S. Yamauchi, M. Kawamura, K.H. Kim and T. Kiba, *J. Vac. Sci. Technol. A,* 36 (2018) 02C102.
11. S. Agrawal, A. Parveen and A. Azam, *J. Lumin.,* 184 (2017) 250.
12. Y.R. Park and K.J. Kim, *J. Cryst. Growth,* 258 (2003) 380.
13. T.Ç. Taşdemirci, *Chem. Phys. Lett.,* 738 (2020) 136884.
14. J.H. Lee, Y.W. Noh, I.S. Jin and J.W. Jung, *Electrochim. Acta,* 284 (2018) 253.
15. L. Zhang, H. Xia, S. Liu, Y. Zhou, Y. Zhao and W. Xie, *Nanoscale Res. Lett.,* 16 (2021) 83.
16. D. Xu, D. Fan and W. Shen, *Nanoscale Res. Lett.,* 8 (2013) 46.
17. X. Niu, H. Wei, K. Tang, W. Liu, G. Zhao and Y. Yang, *RSC Adv.,* 5 (2015) 66271.
18. N. Li, L. Zhang, J. Zhou, D. Jing and Y. Sun, *Dalton Trans.,* 43 (2014) 11533.
19. D.P. Dubal, D.S. Dhawale, R.R. Salunkhe, V.S. Jamdade and C.D. Lokhande, *J. Alloys Compd.,* 492 (2010) 26.
20. S.K. Meher, P. Justin and G. Ranga Rao, *Nanoscale,* 3 (2011) 683.
21. D. Zha, H. Sun, Y. Fu, X. Ouyang and X. Wang, *Electrochim. Acta,* 236 (2017) 18.
22. X. Dong, Y. Cao, J. Wang, M.B. Chan-Park, L. Wang, W. Huang and P. Chen, *RSC Adv.,* 2 (2012) 4364.
23. M-J. Deng, C-C. Wang, P-J. Ho, C-M. Lin, J-M. Chen and K-T. Lu, *J. Mater. Chem. A,* 2 (2014) 12857.
24. Z. Wu, X.-L. Huang, Z.-L. Wang, J.-J. Xu, H.-G. Wang and X.-B. Zhang, *Sci. Rep.,* 4 (2014) 3669.
25. Z. Yang, X. Zhu, K. Wang, G. Ma, H. Cheng and F. Xu, *Appl. Surf. Sci.,* 347 (2015) 690.

26. A. Yavuz, P.Y. Erdogan, N. Ozdemir, H. Zengin, G.Zengin and M. Bedir, *J. Mater. Sci.: Mater. Electron.,* 30 (2019) 18413.
27. K. Lee and W.C. Jung, *J. Korean Phys. Soc.*, 45 (2004) 447.
28. J. Shi, L. Lai, P. Zhang, H. Li, Y. Qin, Y. Gao, L. Luo and J. Lu, *J. Solid State Chem.*, 241 (2016) 1.
29. D.S. Dalavi, M.J. Suryavanshi, D.S. Patil, S.S. Mali, A.V. Moholkar, S.S. Kalagi, S.A. Vanalkar, S.R. Kang, J.H. Kim and P.S. Patil, *Appl. Surf. Sci.*, 257 (2011) 2647.